2
Literature Review

This chapter presents a review of research work reported in the literature. This chapter presents aspects of power quality (PQ) associated with renewable energy, challenges and international standards, especially wind energy sources. Distributed-FACTS devices are emerging as solutions to challenges discussed in this chapter. The role of conventional and adaptive control algorithms are discussed for PQ improvement and optimal switching of DSTATCOM. The identified research gaps are also presented in the conclusion of this chapter.

2.1 POWER QUALITY

Electric power quality refers to the ability of smart electrical equipment to consume the electric power being supplied to it and maintain the voltage within the acceptable range. Also, the various power quality disturbances and the relevant international standards are discussed in the following subsections.

2.1.1 Power Quality Disturbances

The PQ disturbances can be defined as any deviation in voltage, current, and frequency from its acceptable range, resulting in mal-operation and failure of smart electric equipment [Chawda and Shaik, 2019]. The primary effects of PQ disturbances include voltage sag or voltage dip, voltage swell, voltage spikes, voltage fluctuations, harmonics distortion, voltage unbalance, over-voltage, under-voltage, and power frequency variations, very short and long interruptions. The commonly observed PQ disturbances, their symptoms, causes of occurrence of these disturbances, their impacts on equipment and possible mitigation approaches are detailed in Table 2.1.

2.1.2 Power Quality Associated with RE Penetration

Renewable energy penetration into the utility grid would further worsen the PQ, which significantly affect the performance of the system [Chawda *et al.*, 2020]. The specific PQDs associated with RES operating conditions like grid synchronization, High penetration levels, outages, islanding, variations of solar insolation and wind speed variations, strength of AC grid and connected loads are well researched in [Mahela *et al.*, 2020; Shaik and Mahela, 2018; Mahela and Shaik, 2017; Mahela *et al.*, 2020; Al-Shetwi *et al.*, 2020], which have to be detected classified and mitigated accurately. These are summarized as follows:

1. **Grid Synchronization of RES**: The grid synchronization of RES generates PQDs like voltage sag or voltage dips predominantly. During the grid synchronization, a sudden decrease in voltage occurs, termed as voltage dips. The limiting dip value is less than 3%. It is caused by the inrush current produced due to small inevitable differences between the voltage of solar-PV and grid with solar energy penetration. In the case of WE, the reactive power drawn by DFIG causes voltage sags. In the case of hybrid RES sources, voltage swell is followed by voltage sag. Also, voltage rise occurs at the PCC due to the tripping of loads, the phase angle

Table 2.1: Symptoms, Causes, Impacts and Solutions of power quality disturbances in utility grid.

PQ Disturbances	Details
Voltage sag or dip	**Description**: The RMS voltage level decreases between 10-90% of nominal voltage for ½-cycle to 1-minute. **Symptoms**: Memory loss and data errors, equipment shutdown, decreased equipment life and flickering lights. **Causes**: Faults on the utility system, start-up of large motors, inductive loading and switching on the large loads. **Impacts**: Malfunction of embedded based equipment, personal computers, programmable logic controls, and tripping of sensitive equipment. **Solution**: DVR, DSSC, static transfer switch.
Very short Interruptions	**Description**: Complete loss of electrical supply for a few milliseconds to 1 second. **Symptoms**: Decreased equipment life and Flickering lights. **Causes**: Automatic opening and reclosing of protection devices of utility network and life of sensitive equipment. **Impacts**: Tripping of sensitive equipment and electromechanical relays and malfunctioning. **Solution**: Machine-Generator set, DSSSC, DVR, static transfer switch.
Long Interruptions	**Description**: Complete loss of electrical supply for a duration greater than 1-2 sec. **Symptoms**: Loss of supply to customer equipment and computer shutdowns. **Causes**: Equipment failure, trees, fire, vehicles striking to lines or poles, failure of protection device and circuit breaker tripping. **Impacts**: Equipment shutdown and sudden damaging occurred in sensitive equipment. **Solution**: DVR, UPQC, Machine-Generator set, DSSSC.
Voltage spike	**Description**: Abrupt rise or fall of the voltage value for a short duration ranging from several microseconds to few milliseconds. **Symptoms**: Flickering lights, data loss and interference. **Causes**: Lightning, lagging PF, capacitor switching and phase faults. **Impacts**: Destruction of electronic components, tripping of sensitive equipment, damage to insulation and winding. **Solution**: DVR, DSSSC, UPQC.
Voltage swell	**Description**: The RMS voltage level increases to 110%-180% of nominal voltage, at the power frequency for duration of ½-cycle to 1-minute. **Symptoms**: Memory loss and data errors, equipment shutdown, decreased equipment life and flickering lights. **Causes**: Switch ON and switch OFF heavy loads, transformers regulation is affected during off-peak hours. **Impacts**: Loss of efficiency in electric rotating machines. **Solution**: DSVC, DSTATCOM, DVR, UPQC.
Harmonic Distortion	**Description**: Superposition of various sine waves into distorted waveform with different phase, magnitudes and multiples of power frequency. **Symptoms**: Electrical equipment/wiring overheated, the decreased performance of the equipment, improper operation of relays. **Causes**: Arc furnaces, welding machines, weak AC grid, non-linear loads, integration of renewable energy sources and rectifier. **Impacts**: Increase neutral current, nuisance tripping of thermal protections, mal-operation of sensitive equipment, overheating. **Solution**: Active and passive filters, multi-pulse configuration.
Voltage Fluctuation	**Description**: Voltage oscillations with amplitude modulation at a frequency of 0 to 30 Hz. **Symptoms**: Dim or bright lights, speed variation of dynamic loads, overheating of equipment and reduced life of the equipment. **Causes**: AC drives, unbalanced loads, inter-harmonic current components, welding and arc furnaces. **Impacts**: Flickering of lighting, fluorescent and incandescent lamps. **Solution**: DSVC, DSTATCOM, DVR, UPQC.
Voltage Unbalance	**Description**: Unevenness in voltage magnitude with varying phase angle. **Symptoms**: Overheating of equipment, reduced efficiency and speed variation in motors. **Causes**: Large 1-phase loads mainly due to the furnaces load, traction load, unbalanced loads and location of grid-tied RES s. **Impacts**: 3-phase induction machines, overheating in motors and life of the equipment. **Solution**: DSVC, DSTATCOM, DVR, UPQC.
Over voltage	**Description**: A condition in which the voltage value exceeds the rated design limit. **Symptoms**: Dim or bright lights, equipment shut down, over heatings of equipment and reduced efficiency. **Causes**: Unbalanced and balanced load switching, capacitor switching and system voltage regulation. **Impacts**: Overheating in motors, mal-operation of sensitive equipment, relays and life of the equipment. **Solution**: DSVC, DSTATCOM, DVR, UPQC.
Power frequency Variation	**Description**: Any deviation in the fundamental frequency. **Symptoms**: Dim or bright light, heating, reduced efficiency and motors run slower. **Causes**: Usually caused by failure of the generator, extreme loading conditions **Impacts**: Logic-based systems may fail and massive power failure in the grid. **Solution**: DSVC, DSTATCOM, DVR, UPQC.
Under voltage	**Description**: A condition in which the voltage reduces below the rated value of the power system equipment. **Symptoms**: Dim or bright lights, equipment shut down, reduced efficiency, distortion and malfunctioning. **Causes**: Heavy network loading, loss of generation, power factor variation, lack of Var support. **Impacts**: All equipment without backup supply facilities shut down in this condition. **Solution**: DSSSC, DSTATCOM, DVR, UPQC.
Other possible solution	Proper earthing of equipment, energy storage systems, network equipment and design, online or hybrid UPS [Lin and Domijan, 2005].

ϕ, line impedances and X-R ratios. Flickers, impulsive transients, high magnitude oscillatory transients, and low magnitude harmonics are also reported. The frequency deviation increases with the penetration level of RES but is less for solar when compared to the WE source.

2. **High RE Penetration Levels**: The high RE penetration into the ac grid generates harmonics, reactive power, flicker, voltage and frequency based PQ issues. During the high penetration of SPV sources, a sudden decrease in voltage occurs due to small inevitable differences between solar PV and the grid voltage. The DFIG based wind turbine draws high reactive power and is referred to as a significant cause of voltage fluctuation. The frequency deviation increases with the penetration level of RES but is less for solar when compared to the WE source.

3. **Outage of RES**: The outage of RES is associated with voltage variations like swell and sag. The outage of solar-PV does not produce a flicker but has an impulsive transient and frequency variations associated with it. Similar disturbances have been found in the case

of wind and hybrid based RE sources. The frequency drop is directly proportional to the penetration level of RES. Thus, frequency variations can be observed easily when a large outage occurs. Also, the frequency variation is less for WE when compared to solar base RE sources. Low magnitude oscillatory transients are also reported for all types of RE sources.

4. **Islanding of RES**: Islanding causes specific PQDs like voltage sags, swells and low magnitude impulsive transients for solar RES, wind and hybrid sources. Oscillatory transients PQ disturbances are not reported significantly for islanding with RE sources, requiring more focus. This event is also associated with a sudden increase in frequency, unlike outage or grid synchronization. The frequency jump is more in the case of either solar or wind when compared to the islanding of sources simultaneously.

5. **Variation of Solar Insolation**: A decrease in solar insolation creates voltage sag. The voltage fluctuations are also observed with variations in the voltage magnitude. These also indicate the presence of low magnitude flicker in the voltage with low magnitude transients. Due to sudden change in the solar insolation, frequency deviations occur, current and voltage harmonics increase with an increase in the penetration level of solar PV base RE sources.

6. **Variation of Wind Speed**: Wind speed variations also cause voltage fluctuations, which produces a low magnitude flicker. The transient magnitude, frequency deviation, current, and voltage harmonics increase when WE penetration rises. The voltage variations and ripples also indicate the presence of low magnitude flicker in the voltage in the case of variation of wind speed and solar irradiation changes.

7. **Strength of AC grid**: The higher line impedance value leads to low SCR, which is primarily responsible for the weak grid. Hence, the voltage and frequency at PCC are observed weaker in the rural grid and limit the WE penetration levels.

8. **Presence of loads**: The unbalanced loads of a three-phase line are generated due to the unequal three-phase line, or open-circuited one-two phase of a line. These loads cause unbalanced 3-phase currents, which raises an unstable 3-phase terminal voltage. Also, in the case of non-linear loads, the current signal contains harmonics and significantly deteriorates the system's PQ. Consequently, weak grids in the presence of these loads can pose severe PQ disturbances and limit the RE penetration levels at PCC.

These PQDs, and the sources of disturbances like the operating conditions of RES along with power system faults, if not detected and mitigated quickly, might cause the failure of the end-use equipment and also power system assets [Chawda and Shaik, 2019; Li and Reinmuller, 2020; Pal and Panigrahi, 2020; Abdelsalam *et al.*, 2020]. Hence, IEEE has laid down the guidelines, which is measured based on the PQDs as mentioned above in the utility grid with RE penetration [Green and Wind, 2000]. These PQDs majorly influence the performance of the RE sources during grid operating conditions causing voltage and frequency instability at PCC and hence, restricting the RE penetration level into the utility grid. Therefore, researchers should reconsider or modify the PQD mitigation techniques in the presence of RE sources. Presently, mathematical, simulation and experimental languages such as C, matrix laboratory (MATLAB), electromagnetic transient design and control (EMTDC), Power system computer-aided design (PSCAD), and very high speed integrated circuit hardware description language (VHDL) are generally employed for parametric synthesis based generation of PQ disturbances [Lin and Domijan, 2005; De and Debnath, 2017; Achlerkar *et al.*, 2018].

2.1.3 International Standards for Power Quality

International bodies such as the Institute of Electrical and Electronics Engineers (IEEE), European Committee for Electrotechnical Standardization (CENELEC) and International

Table 2.2: Important international standard of power quality.

Org.	Standards	Illustration
IEEE	2030-2011	Guidelines for for Smart Grid Inter-operability of energy technology, end-use applications, and loads.
	3002.3-2018	Guidelines for short-circuit studies and analysis of industrial and commercial power systems
	1204-1997	Guidelines for a weak grid in the system is defined as SCR
	519-2014	Updated guidelines for harmonics control of electrical PQ
	1159-1995	Guidelines for monitoring of electrical PQ issues
	P1433	Power Quality definition
	1159.3-2003	Guidelines for the transfer of Power quality data
	1100-1999	Guidelines for powering and grounding of sensitive equipments
	1250-1995	Guidelines for service to sensitive equipment from momentary voltage disturbances
	1366-2012	Guidelines for electric power utility indices
	1250-2011	Guidelines for identifying and improving voltage quality in power systems
	P1409	Guidelines for PQ improvement in utility network using custom power technologies.
	P1547-2003	Guidelines for interconnecting DG/RES in utility network
	P1547.1-2020	Updated guidelines for interconnecting DG/RES in utility network
	929-2000	Guidelines for compatible operation of grid tied-SPV.
IEC	60909	Guidelines for R/X ratio calculation
	61000-2	Guidelines for design requirements of small wind turbines
	61000-2-2	Guidelines for maintaining compatibility with low frequency disturbances in utility network
	61400-27	Guidelines for electrical simulation models of wind turbines
	61400-21	Guidelines for power quality requirements for grid connected Wind Turbines
	61400-13	Guidelines for measuring power for grid connected Wind Turbines
	61400-3-7	Guidelines for measuring of emission limits for fluctuating loads
	61000-2-4	Guidelines for compatibility level in industrial plants for low frequency disturbances
	61000-4-7	Guidelines for non-linear distortion in utility network
	61000-4-15	Guidelines for measurement of voltage flicker
	61000-4-30	Guidelines for minimum accuracy for measurement of different electrical parameters
	1052-2018	Guidelines for specifications of STATCOMs
	62927	Guidelines for testing of STATCOM
EN	50160-1999	Guidelines for voltage characteristics of utility network
	50308	Guidelines for wind turbine protective measures, design requirements, operation and maintenance.

Electrotechnical Commission (IEC) are continuously coordinating with each other to standardize the PQ at grid level [Association *et al.*, 2009]. These organizations provide various international PQ standards, which help regulate the PQ with and without RE penetration. The guidelines for power loss analysis with SPV penetration are proposed in [Wu *et al.*, 2011]. The IEEE standard 519-1992 helps to understand harmonics in power system network [Blooming and Carnovale, 2006; F II, 1993]. IEEE-P1547 standard states that voltage fluctuations must be less than $\pm 5\%$, and the amount of DC content must be less than 0.5% of total output current at the PCC [Basso and Deblasio, 2003]. The harmonics voltage and current limits for different voltage levels are updated in IEEE standard 519-2014 [C-2, 2014]. This updated standard significantly focused on harmonic measurements and introduced the statistical evaluation in brief and short time-harmonic measurements. It can be perceived from IEEE standard 519-2014 that the voltage distortion level decreases with an increase in voltage level, and current harmonics limits depend on the short circuit strength of the system. The relevant IEEE standards related to PQ and RE penetration into the utility grid are presented in Table 2.2. The tabulated data are collected from [C-2, 2011, 2018a, 1997; Association *et al.*, 2009; F II, 1993; Basso and Deblasio, 2003; C-2, 2020, 2014; Green and Wind, 2000; Sabin and Sannino, 2003; Emanuel *et al.*, 2009].

2.2 STATE OF ART-WIND ENERGY SYSTEMS

Wind power with the interfacing of power electronics is growing as innovation brings down costs and starts to guarantee a green and clean energy future. The continuous enhancements in these sources added features like small installation, accommodates grid flexibility, running cost, maintenance less operation, low power loss, meeting load demand with high-quality power.

Wind Energy is a cornerstone of achieving net-zero and powering a green recovery as a cost-competitive, resilient power source with the most decarbonisation potential per MW. Thus, worldwide new installation of WE source is observed 93 GW with a 53% yearly increment addition in 2020. The present global wind power capacity is observed as more than 740 GW [Council, 2017].

Several countries and certified agencies have reached relatively high WE penetration levels in their distribution networks. However, testing documents on the strength of the grid, connected loads with high WE penetration levels are not available.

The country-wise new installed capacity of the Onshore WE source in 2020 is recorded at 48,940MW in China, 16,913 MW in the US, 2,297 MW in Brazil, 1,532 MW in Norway, 1,431 MW in Germany, 1,400 MW in Spain, 1,317 MW in France, 1,224 MW in the Turkey, 1,119 MW in India, and 1,097 MW in Australia. However, the cumulative capacity is recorded at 278,324 MW in China, 122,275 MW in the US, 55,122 MW in Germany, 38,625 MW in India, 27,238 MW in Spain, 17,946 MW in France, 17,750 MW in Brazil, 13,731 MW in the United Kingdom, 13,578 MW in Canada, and 10,543 MW in the Italy [Council, 2017].

Similarly, The country-wise new installed capacity of the Offshore WE source in 2020 is recorded at 3,060 MW in China, 1,493 MW in the Netherlands, 706 MW in Belgium, 483 MW in the United Kingdom, and 237 MW in Germany. However, the cumulative capacity is recorded at 10,206 MW in the United Kingdom, 9,996 MW in China, 7,728 MW in Germany, 2,611 MW in the Netherlands, and 2,262 MW in Belgium [Council, 2017].

Specifically, India is the world's fourth-largest energy consumer and is committed to limiting global warming in steps. The renewable energy target of India is 175 GW by 2022 includes 60 GW onshore WE. As of February 2021, 39 GW of wind capacity was installed, comprising 10.25% of the power mix. The government of India has also shared its vision for longer-term RE targets of 450 GW by 2030, including 140 GW of wind [Council, 2017].

The present scenario of higher levels of wind energy penetration by the independent system operators (ISOs) is illustrated in Fig. 2.1 (Source: AWEWA, SPP, ERCOT, MISO, CAISO, NYISO, ISO-NE, PJM, Berkeley lab). WE penetration (represented as a percentage of connected loads) had been recorded at 23.9% in the Southwest Power Pool (SPP), 18.6% in the Electric Reliability Council of Texas (ERCOT), 7.3% in both the Midcontinent Independent System Operator (MISO) and the California Independent System Operator (CAISO), 2.8% in ISO New England (ISO-NE), 2.7% in the PJM Interconnection (PJM), and 2.5% in the New York Independent System Operator (NYISO). However, the WE capacity in the global power market significantly increased, with the most impressive numbers in SPP (25%), the Mountain region (16%), the Midwest (16%). The smaller number is observed in the Northwest (7%), with no plan in the Southeast by the end of 2018 [AWEA, 2018; Bórawski *et al.*, 2020].

Multiple attempts have been compelled to extend the Wind Energy Conversion System (WECS). These generating topologies are described as type-1 (limited variable speed), type-2 (limited variable speed), type-3 (the variable speed with partial power electronics conversion), and type-4 (the variable speed with full power electronics conversion).

1. **Type-1 WECS system** Type-1 Wind Energy Conversion System (WECS) is illustrated in Fig. 2.2. The significant features of this generating system are as follows:

    - Squirrel-cage Induction Generator (SCIG) combined straight to the transformer.
    - The turbine speed is fixed to the grid frequency.
    - The turbine shaft rotates faster than the grid frequency and produces a negative slip for generating active power.

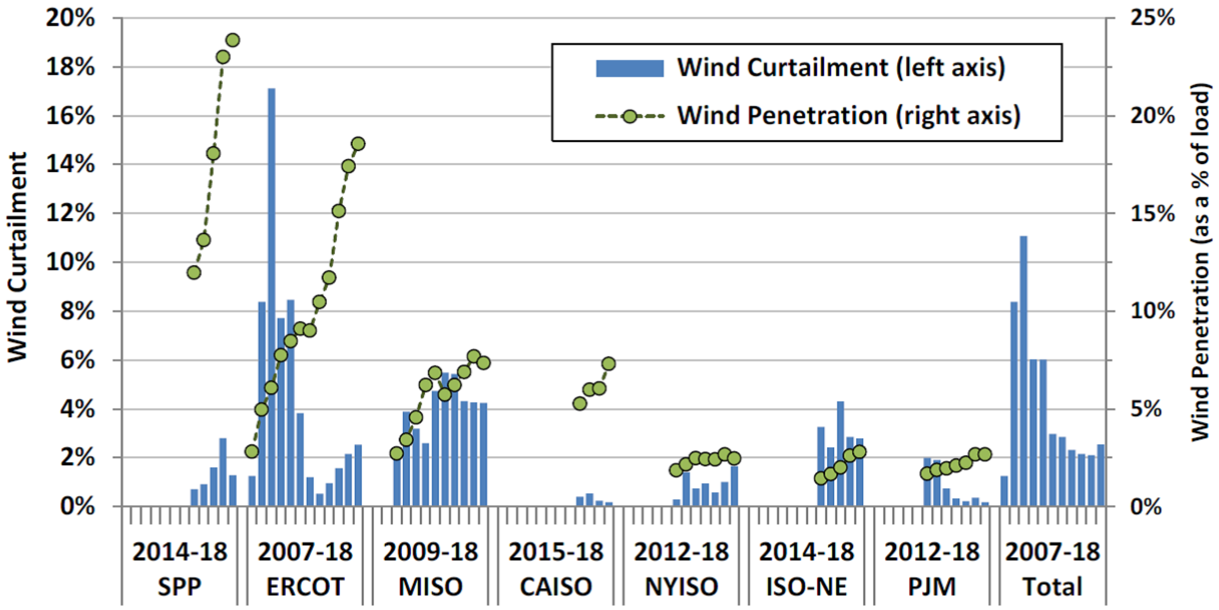

Figure 2.1: Present scenario of WE penetration levels by ISOs (Source:Berkeley lab).

- The turbine's operating speed under controlled conditions is a nearly linear function of torque when speed is fixed.
- The mechanical inertia of the drive train can restrict the rate of change in electrical output during the variable speed.

Merits: Simple, low cost and low maintenance.

Demerits: High mechanical stress, weak voltage stability, and challenging to control.

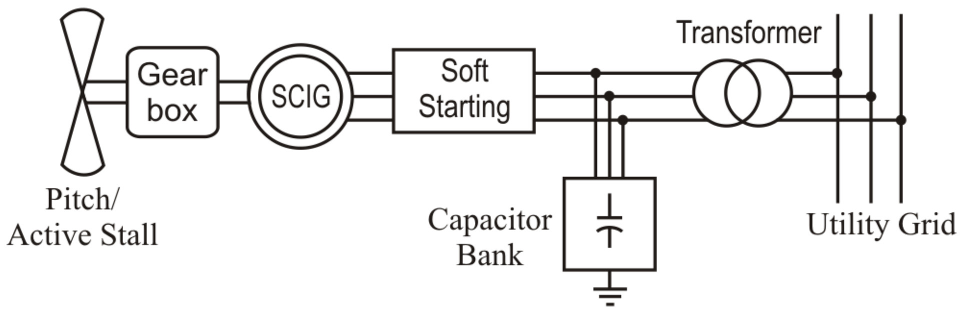

Figure 2.2: Wind energy conversion system with Type-1 and Type-2 configuration.

2. **Type-2 WECS system** Type-2 Wind Energy Conversion Generating (WECS) system is illustrated in Fig. 2.2. The significant features of this generating system are as follows:
   - Wound rotor induction generators (WRIG) are combined right to the WECS, similar to Type 1. However, it is added one additional variable resistor in the rotor circuit.
   - This additional resistor helps control the rotor currents very fast to maintain continuous power.
   - It can also affect the machine's dynamic response under grid interruptions.

Merits: Simple, low cost and low maintenance.

Demerits: High starting inrush, weak voltage stability, and challenging to control.

3. **Type-3 WECS system** Wind Turbine (WT) with Doubly Fed Induction Generator (DFIG) is an advanced WT system used in the WECS system because it has low investment and flexible control characteristics. The schematic diagram of the Type-3 DFIG-based WECS system is illustrated in Fig. 2.3. A DFIG is a wound rotor induction generator with the stator connected to the grid directly and the rotor attached to the system by a back-to-back converter. The rotor side converter (RSC) aims to control the active and reactive power on the grid individually. In contrast, the grid side converter (GSC) or built-in converter maintains the dc-link voltage at reference value using the appropriate control scheme. The significant features of this generating system are as follows:

   - Doubly Fed Induction Generator (DFIG) design is next level WEG system, by combining variable frequency ac excitation to the rotor circuit.
   - The new rotor excitation is furnished through slip rings by VSC, which regulates the current by adjusting magnitude and phase angle.
   - This rotor-side converter (RSC) is combined with a grid side converter (GSC), which transfers electric power instantly with the grid.

   Merits: Good conversion efficiency, reasonable control of powers.

   Demerits: Weak voltage stability, weak fault ride-through capability, challenging to control, sizeable short circuit contribution, damage during the improper synchronization, required specific reactive power support, high stress on the rotor, and gearbox under unbalancing.

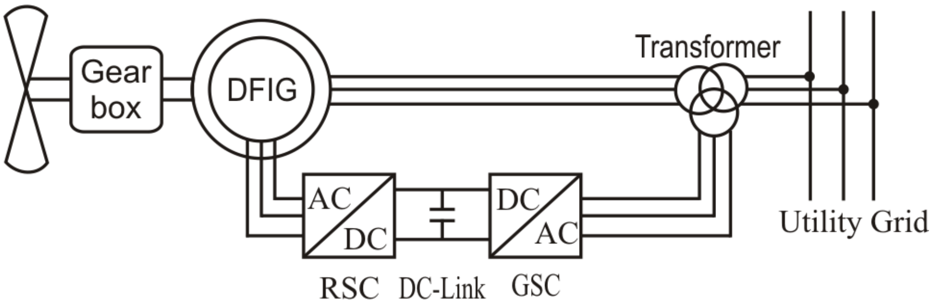

Figure 2.3: Wind energy conversion system with Type-3 configuration.

4. **Type-4 WECS system** Type-4 Wind Energy Conversion System (WECS) is illustrated in Fig. 2.4. The significant features of this generating system are as follows:

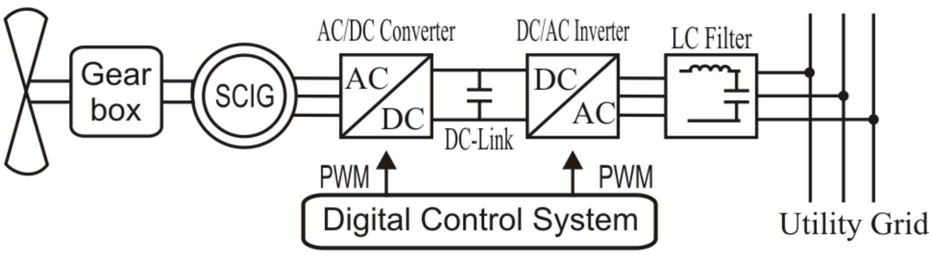

Figure 2.4: Wind energy conversion system with Type-4 configuration.

- The full AC-AC converter design is also considered a next-level WECS system as it provides flexibility in smooth operation.
- The output power of the RSC is directly sent through the DC link capacitor to the GSC.
- The turbine is permitted to rotate at its optimal aerodynamic speed for smooth operation.
- The rotor drives gearbox in the geared system to increase generator shaft speed.
- The gearbox is eliminated in the direct driven for generating specified frequency well below the grid.
- Type-4 WECS system can be used wound rotor synchronous machines, permanent magnet synchronous machines, or squirrel cage induction machines, based on the design consideration of the specific application.

Merits: Voltage stability and fault ride-through capability, flexibility and fast operation, control on short circuit currents, frequency and voltage

Demerits: Fault current contribution is restricted, and reactive power support is comparable to the synchronous machine.

These WECS systems are generally used as Wind Energy sources either in isolated or grid-connected modes. However, integrating WE sources into the grid generates many issues such as power forecasting, low voltage ride-through, protection, the strength of the AC grid, reactive power capability, harmonics, voltage stability, frequency stability, small-long signal stability, etc. [Ahmed *et al.*, 2020; Chawda *et al.*, 2020].

2.2.1 Challenges Associated with WE Penetration

This section covers the emerging challenges associated with higher levels of WE integration into the remotely located grids that must consider maintaining the security and power quality of the distribution network.

1. **Power Forecasting Challenge** Forecasting of the output power of the WES has been observed very helpfully for distribution power system supervision. It has been perceived that there is no ideal approach for forecasting WE output power due to the unpredictable nature of the wind. However, during higher levels of WE penetration, the forecast performs a notable role in decreasing the expenses of electric power generation. Moreover, unpredictable disturbances of ramps can reduce the security of the remotely located network. In this regard, the literature suggested some methods for forecasting data using historical data. The forecast methods are the deterministic forecast (DF) method and uncertainty analysis (UA) method.

   The deterministic forecast (DF) method includes physical DF, statistical DF, intelligent DF, and hybrid DF. The physical DF strategy utilized climate data like temperature, altitude, terrain, etc. These data are collected from the multiple research stations scattered in geographic regions or virtually designed using dynamic equations. Also, the statistical DF is a time series based strategy and utilizes historical statistics, probabilities, and stochastic data. In continuation, intelligent DF strategies are generally used historical weather data for future forecasting of WE output. However, the uncertainty analysis (UA) utilized three approaches: probability prediction, risk indices, and generation scenarios for predicting the output power of the WE sources in remote areas. Moreover, the mathematical functions have been developed using the power curves for the precise explanation of the wind speed versus the output power of the WE [Foley *et al.*, 2012].

2. **Low Voltage Ride-through Challenge** The ability of wind energy conversion system (WECS) to continue integrated into the distribution grid in the event of under-voltage issues is termed as low-voltage ride-through (LVRT). A shutdown of the high capacity of WEG farms become a critical influence on transient and steady-state stability of remotely located grid control. Consequently, the study of LVRT is a basis for WECS under the faulty events of the grid. This system needs to resist voltage interruptions without getting disconnected from the remote grid. Concurrently, the international standards state that the requirement of voltage to attain 80% of the nominal value within 0.5 seconds and 95% within 15 seconds after the fault removal at the PCC [Mahela *et al.*, 2019]. This is one of the significant challenges associated with high WE integration, which needs to be more focused and addressed effectively to the perceived objectives mentioned above. Thus the continuous requirement of new research works for specific design under such conditions with matching grid codes and incorporated LVRT schemes.

3. **Power Quality Challenges**

    - **Voltage/Reactive power support** The induction generators are generally utilized in the WECS systems, requiring reactive power for excitation. Thus, they have not advantaged of reactive power support like the synchronous generators. It has been recognized that when modern technologies are associated with the higher levels of generations and loads, maintaining the voltage is always a major challenge. Therefore, the operation of higher levels of WE generation is a significant cause of high voltage fluctuations and voltage flickers. Besides, the strength of the AC grid also provides considerable impact during more elevated levels of WE integration, as it requires continuous voltage support at the PCC. These issues have been investigated with the wind side converter in the past. But due to the rating issue of these sources, wind side converter rating also recognized less. Therefore, this converter's capacity of reactive power injection is found limited to meet the reactive power demand of non-ideal grids. Hence, this also may affect the WE penetration levels. However, the proportion of WE in the distribution system shouldn't exceed 20% [Kroposki, 2017].

      It has been observed that to maintain the rated power of the WE source, the additional inverter is essential to fulfilling the reactive power demand. Therefore, the necessity of an additional inverter named D-FACTS devices is increased to support the voltage of weak grids during the higher levels of WE penetration.

    - **Frequency Support** With the continuous expansion of WECS technology, grid-tied WE source capacity progressively increases, which dangerously influences the frequency stability of the distribution grids. The DFIG is mainly utilized worldwide due to its simple operation, good controllability and cost. However, the WECS turbine converter decouples the fan rotor speed from the system frequency. Therefore, systems equivalent inertia is continuously reducing because the WECS turbine does not provide system inertia. In addition, higher levels of WE penetration also dangerously influence the frequency stability of the remotely located grid due to interfacing converters. This is one of the critical reasons that most countries have a limited penetration rate.

      One of the solutions found in the literature is the inertial frequency response (IFR). The IFR generally receives strength from the rotating masses to resist a frequency variation from the acceptable frequency range. In continuation, the primary control named automatic governing system is initiated to maintain the frequency variations within the standard range. Later, the secondary control also helps restore the system frequency under the stipulated limit. Energy storage devices, DFACTS devices, their control, and load control can also be suitable alternate solutions for frequency degradation challenges [Attya *et al.*, 2018].

- **Harmonics** Integration of higher levels of WECS system into the grid, primarily remotely located grid injects current and voltage harmonics due to power electronics-based devices and interfacing converters. Ensuring these harmonics under the permissible limit is one of today's most critical challenges. The IEC 61000-3-2, 1159 and IEEE-519-2014 international standards address the allowable limits of harmonics distortion. The estimation of harmonics in a remote location is rigid when higher levels of WECS are integrated. The grid is weak at this PCC, and voltage and current harmonics are already present in the system. Also, at this point of contact, the wave shape is not sinusoidal, and the current is not in phase with the voltage means a low power factor. Hence, it has been found that harmonics voltages are always present in the grid. These harmonics include integer harmonic of 5^{th} and 7^{th} order, affecting the estimations. It has been recognized from the literature that the self-commutated pulse width modulation inverter is included in the variable speed WECS turbines. This system's advantages are that it controls active and reactive power as per the given rating. The disadvantage of this system is producing a harmonic current. Hence, researchers have started implementing filters like LC resonant passive filters. However, these filters have the disadvantages of considerable size, fixed compensation, and resonance [Chawda *et al.*, 2020].

  The solution finds in the literature is the active utilization of D-FACTS devices. These devices can mitigate all types of PQ issues, especially harmonics.

- **Flicker** Flicker has widely been considered a power quality issue in the grid-tied-WECS system. A grid-tied variable-speed WECS system generates it with interfacing converters, variations in output power, wind shear, grid strength, wind tower shadow and characteristics of the WECS. Fluctuations in voltage cause it due to load flow variations in the grid. It may restrict the higher penetration levels of the WCEG system in grid-connected mode. However, variable-speed WECS has exhibited more excellent performance for flicker emission in association with fixed-speed WECS system. It has been recognized from the literature that flickers are generated in a fixed-speed WECS system when it reaches maximum speed. However, a large-size WECS turbine generates a lower flicker compared to a small-size WECS turbine. Meanwhile, the flicker level can be observed by amplitude, shape and frequency components of the fluctuated voltage waveform based on the flicker meter defined in IEC 61000-4-15.

  Literature also suggested some solutions to overcome this PQ issue. These include reactive power compensation, active power curtailment, voltage and frequency regulation, and maintaining the DC link voltage of the built-in converter.

4. **Angular Stability Challenge** The angular stability is also termed inter-area oscillations. The strength of the interfaced devices in the distribution system is to stay synchronized during specified or unspecified disturbances. It has been observed from the literature that, Small-signal stability is continuously increased during the higher levels of WE penetration and may introduce angular instability due to reactive power issues. Also, some researchers concluded that the higher the WE penetration levels into the grid, the lower the inertia, which may lead to collapsing the system. Hence this specific challenge needs more focus at higher levels of WE integration [Gautam *et al.*, 2009].

5. **Protection Challenge** Protection is a significant challenge when higher levels of the WE integrate into the remotely located grids. In this connection, the short circuit is a notable cause of distribution network failure as it provides high stress on the connected distribution elements. It has been recognized that types of the WECS system contribute short circuit current (SCC) based on the system design and configurations. These configurations and designs considered the number of WECS systems connected in parallel, their types, connected grid and loads or isolated mode, etc. In addition, one of the most frequent challenges found in

the literature is underreached and overreach issues of relays during the high WE integration. However, the additional protection challenges associated with the remote grids are false tripping/mal-operation, loss of coordination, blinding security, auto recloser difficulties and grid disconnection issue, which are well discussed in [Telukunta *et al.*, 2017].

Protection issues as mentioned above, researchers need to consider new protection schemes, design, implementation methods, unique and fast measurement units, coordination of each connected unites and most crucial modern protection plans. These points quit the solution of protection challenges as mentioned above.

6. **Environmental Challenge** The output power of the WECS system depends on the input speed of the wind, and the speed of the wind highly relies on weather and climate variability. Therefore active power penetration from the WECS system is affected. Wind speed's intermittent nature and seasonal variability also significantly affect the system operation. It has been recognized from the literature that, in multiple areas-regions, in the globe, there is a shift in the wind speed pattern from higher to smaller Wind Velocities (WV). Hence, the appearance of WV more diminutive than the cut-in rate becomes more expected, which appear in lower WE output power [Dai *et al.*, 2015].

   The presently available temporary comprehensive assessment is not enough for climate projections. Hence, there is a strong need for the specific design of wind blades, structure, types, concrete base and interfacing converters, and control based on the wind speed data of different regions-areas from the globe.

2.2.2 Solutions Associated with WE Penetration

The WE sources have accelerated the development of greener energy sources. The rising number of WECS systems necessitates fresh approaches for operating and controlling the remotely located grid to support or enhance the reliability and quality of power. The power electronic-based technology plays an essential role in the grid-tied WECS system. The built-in converter of the WECS system may fail to meet the reactive power demand unless it is considered in the design of the converter. A built-in converter's failure to provide the required reactive power supply may lead to voltage instability and other PQ disturbances. This leads to the limited power injection capability of the WE generator. Therefore, an additional DSTATCOM infrastructure at the Point of Common Coupling (PCC) is suggested in the literature to mitigate the PQ in the above scenario. In addition, a control algorithm that drives the DSTATCOM is also equally important, whose parameters can be tuned as per the changes in system parameters. However, continuous research is going on, and researchers have suggested possible solutions, which are depicted in Fig. 2.5.

1. **Without Energy Storage Based Solution** A grid-tied DFIG based WEG system has been classified into two sections to explain the mechanical and electrical section, which is illustrated

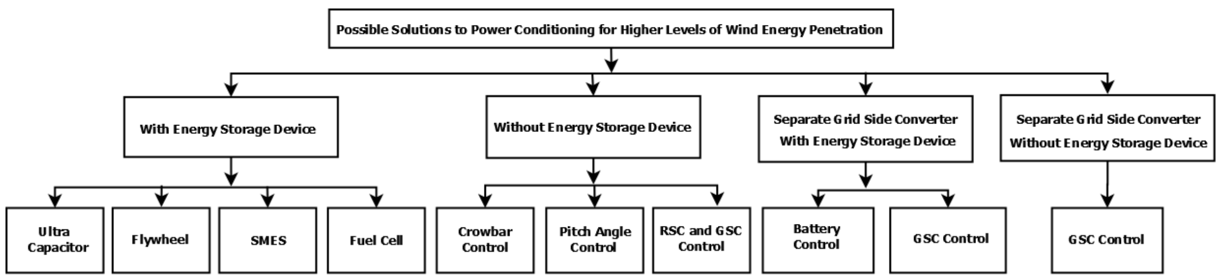

Figure 2.5: Possible solutions of challenges associated with grid-tied DFIG based WECS system.

in Fig. 2.6. The mechanical section of the connected system includes an aerodynamic design with rotor blades and a drive train system. However, the electrical section includes generator and power electronic-based back to back converters, control structure for crowbar control, pitch angle, generator torque, power optimization, frequency, converter etc. Also, RSC and GSC side control has been managed by suitable control techniques and improve the performance of these converters [Mahela and Shaik, 2016]. Hence, grid operators may consider this type of configuration to address various issues and provide possible practical solutions to allow higher levels of WE integration into the remote location grids.

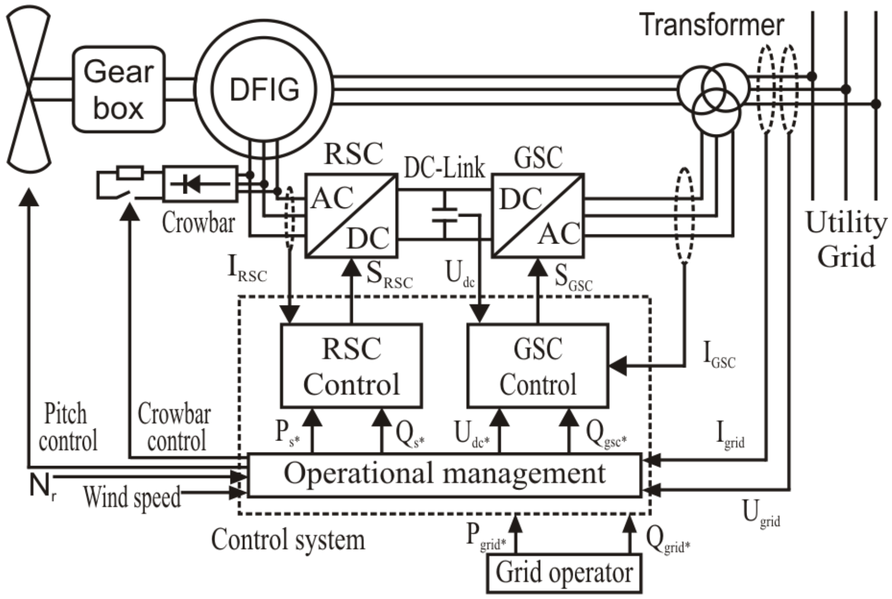

Figure 2.6: Without energy storage based solution.

2. **With Energy Storage Based Solution** One of the vital solutions for the challenges mentioned above is the Battery Energy Storage System (BESS). It is connected with the GSC and injunction with the DC-link capacitor of the back to back converters, as depicted in Fig. 2.7. The benefits of connecting this additional BESS at the DC-link are to provide auxiliary services enhancing dispatching ability. This modified configuration functions as a “shock absorber” for the connected system and includes grid reliability, flexibility and efficiency. Also, most importantly help to integrate higher levels of WE sources into the remotely located grid without any compromise and mitigates peak load demand and price of electrical power during running conditions. It has been observed that The pumped hydroelectric energy storage system (PHESS) and compressed air energy storage system (CAESS) based BESS technologies are vital for large scale applications. However, superconducting magnetic energy storage system (SMES), supercapacitor(SC), Flywheel energy storage system(FESS) have also been the right choice for the remote located WE applications.

3. **Additional Reactive Power Compensator Based Solution** It has been recognized from the literature that, in solution one, RSC and GSC side controls are designed based on conventional methods like vector control, and these controls do not consider the strength of the grid and connected distribution loads. Hence, these controls cannot adopt the changes associated with grid strength and connected loads and fluctuations in the corresponding converters. Also, reactive power management, DC-link control and voltage-frequency stability are significant concerns during synchronization and higher penetration levels of WE sources. Therefore, the concept of an additional reactive power compensator comes into the picture, and recently researchers have focused more on it. The various benefits of the shunt connection of this converter have been investigated in [Chawda and Shaik, 2019]. As per this research, higher levels of WE integration is enhanced by mitigating power quality issues. It has also

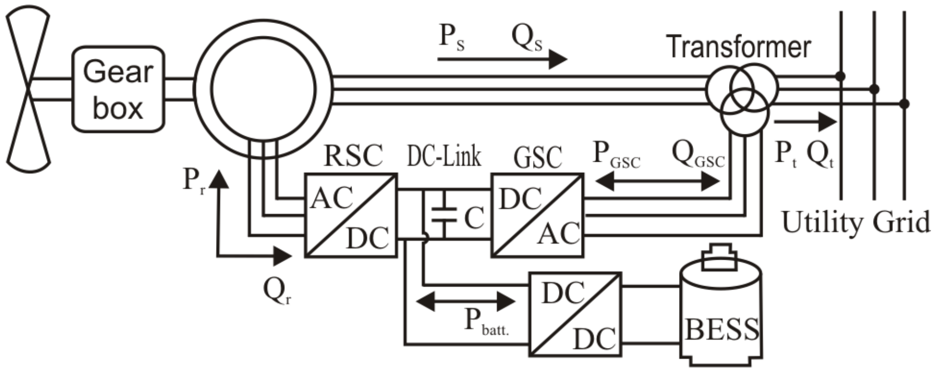

Figure 2.7: With energy storage based solution.

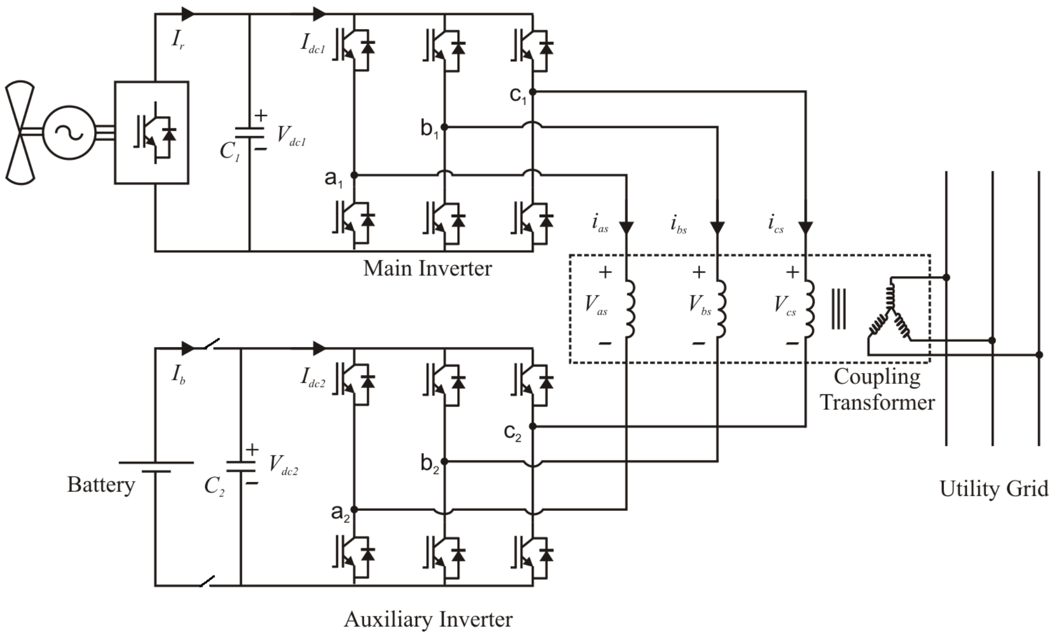

Figure 2.8: Additional DSTATCOM and BESS based solutions.

been found that the integration of an additional reactive power compensator increases the system's initial cost due to the converter rating with a specific application. This particular issue and issues discussed mentioned above are solved by the control algorithm employed. Authors [Chawda and Shaik, 2019] et al. also addressed the control algorithm for this device and designed it to adopt the changes associated with the WE output power, loads, strength of grid, and DC-link voltage. Thereby mitigating the power quality issues and reducing the cost of this converter. The solution of challenges associated with higher levels of WE penetration is as depicted in Fig. 2.8.

In addition, energy storage can also be added to the additional reactive power compensator control to enhance the capability and control of the DC-link capacitor with the additional facility of storing the power, as illustrated in Fig. 2.8, by connecting the switch. Also, the battery energy storage system can be used as a separate source with the interfacing of DC-DC and DC-AC converters. Still, the DC to AC extra converter costs are added with an additional control strategy. Hence the additional reactive power compensator enhances the WE integration levels in remotely located grids by mitigating various power quality issues.

4. **Other Possible Solutions** The other possible solutions are well discussed in [Mahela and Shaik, 2016]. A supercapacitor (SC)-based technique for grid-tied WE applications includes a direct dc-link connection of SC, connection to dc-link through the dc-dc converter, common ac bus connection, and combined BESS and SC connection to dc-link. These all combinations can be designed and implemented based on the application. It also has been noted that possible solutions are not limited, and research on other possible solutions is in the development stage to promote higher penetration levels of Green energy.

2.3 STATE OF ART-DISTRIBUTED-FACTS DEVICES

Distributed-Flexible AC Transmission System (DFACTS) devices are used in the distribution grid to control line impedance, phase angle, current harmonics, voltage harmonics, voltage magnitude and unbalanced loading to maintain power quality. In [Gandoman *et al.*, 2018], a new concept of DFACTS is recommended, which is a promising economical solution to PQDs in a utility grid-tied with RE sources. It also provides many advantages as they are small, less costly, and easier to implement than conventional FACTS devices. The DFACTS devices are efficient in enhancing PQ in the utility grid with RE penetration.

The DFACTS devices are classified into series-connected, shunt connected, shunt-series connected, and series series-connected based on interconnection with utility grid as shown in Fig 2.9. The DFACTS devices' performance for PQ mitigation depends on the different attributes, which are included and discussed in Table 2.3. These attributes of DFACTS devices are beneficial to evaluate performance levels in hardware design.

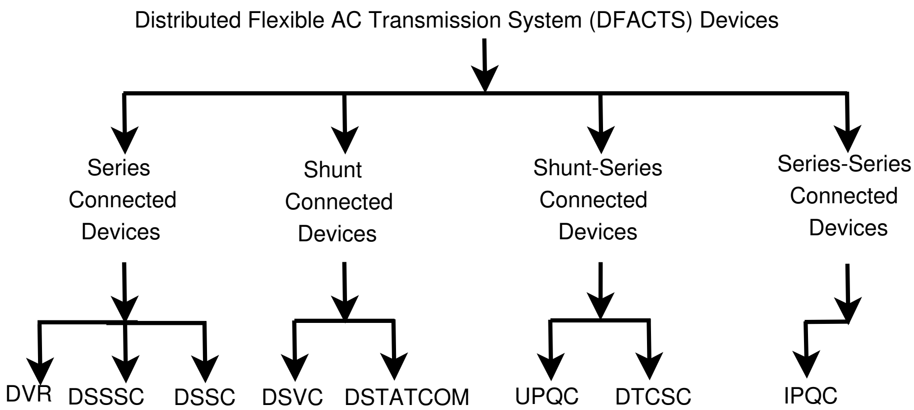

Figure 2.9: Classification of DFACTS devices.

2.3.1 Series DFACTS Devices

These compensators are connected in series with the utility grid. They may have mutable impedance like a capacitor and reactor. Series compensators work on the principle of injecting voltage in series with grid voltage, thereby controlling the real power flow in the utility network. These devices can also be utilized to limit the short circuit current, eliminating the subsynchronous resonance (SSR), reactive power loss, and damping power oscillations. Commonly used series-connected DFACTS devices include DSSC, DSSSC, DVR etc.

Table 2.3: Performance comparison of DFACTS devices.

Attributes	DFACTS devices for PQ improvement			
	IPQC	DSSSC	DSTATCOM	UPQC
Reactive power compensation	Good	Poor	Best	Best
Harmonic suppression	Adjustable	Adjustable	Adjustable	Adjustable
Load balancing	Good	Good	Best	Good
Transient stability	Good	Good	Best	Best
Steady state stability	Good	Good	Best	Best
Voltage control	Good	Good	Best	Best
Power rating of converter	Small	High	High	Small
Number of switches	9-12	6	6	12
Overall cost	Medium	Low	Low	High
Performance level in hardware design	Good	Good	Best	Best

2.3.2 Shunt DFACTS Devices

A shunt compensator is a VSC connected in parallel with the utility grid. It may have mutable impedance and source. Shunt compensators work on injecting current in shunt with grid voltage, thereby allowing power flows by enhancing the voltage profile in the utility network. These devices help maintain power factors, balance the load, mitigate reactive power, reduce harmonics, and provide uninterrupted power. Commonly used shunt connected DFACTS devices include DSTATCOM, DSVC, etc.

2.3.3 Shunt-Series DFACTS Devices

This compensator provides both shunt and series compensation. These are controlled in a co-equal manner using series and shunt elements. In this compensator, the shunt component of the compensator inject current, and the series component of the compensator injects voltage in the utility grid. The dc-link capacitor is utilized for active and reactive power exchange between these compensators. These are effective in improving system stability and mitigating PQ issues with RE penetration. Various shunt-series DFACTS devices include UPQC, DTCSC, etc.

2.3.4 Series-Series DFACTS Devices

Interline power quality compensator (IPQC) is a widely used active and reactive power compensator in utility grid-tied with RE sources. It consists of two branches (inductive and capacitive), which help control active and reactive power independently by adjusting the phase shifter or branch impedance. The IPQC can regulate power flow in both directions and minimise short circuit current to allow active power flow control in the utility network. Combined DFACTS devices are more complex than other devices due to the coordinated control challenge.

2.3.5 Role of DFACTS Devices for Power Quality Mitigation

The controllability and flexibility of Distributed-FACTS devices make them suitable candidates for mitigating PQ disturbances associated with the WE source. Distributed-FACTS controllers aim to provide fast load voltage regulation and the controllable injection or absorption of reactive power at the PCC and succeed PQ enhancement, reactive power compensation, voltage regulation, and enhancement of line capacity during power system abnormalities [Tareen *et al.*, 2018].

RE sources are expected to supply 20–30% of the electrical energy by 2050 from sources that majorly include wind, solar and hybrid RE sources. Also, new designs of Distributed-FACTS devices will target devices such as DSTATCOMs, UPQCs, and DVRs for Modern metropolitan and rural utility networks [Gandoman *et al.*, 2018]. The DSTATCOM with adaptive controls are the new possible solution for improving PQ in the utility grid.

The main advantages of DFACTS for PQ improvement in the utility grid with RE penetration are as follows,

- Enhanced utilization of existing utility grid.
- Increased flexibility and power flow control in a utility grid with RE penetration.
- Enhancement of transient and dynamic stability limit of the utility grid.
- Increased system reliability and security.
- Environmental friendly.
- Increased quality of power supply.

2.4 STATE OF ART ON VARIOUS CONTROL ALGORITHMS

Various control algorithms proposed to estimate reference signals used to control DFACTS devices are broadly classified into two categories, namely frequency-domain (FD) and time-domain (TD) algorithms. The performance of these algorithms is graded based on how fast and accurate reference signals are generated. The frequency-domain based algorithms include recursive discrete Fourier transform (DFT), fast Fourier transform (FFT) and miscellaneous FD based algorithms. These algorithms for power quality mitigation studies are not often used due to their inaccuracy, as reported in [Borkowski *et al.*, 2014]. The TD based control algorithms were found to be suitable for power quality mitigation [Singh *et al.*, 2010]. These algorithms are sub-classified into conventional control and adaptive control algorithms. The existing traditional control algorithm (CCA) are based on Clark transformation of voltage and current signals. However, adaptive control algorithms (ACA) are based on error minimization and weight updation of voltage and current signals. The general classification of various control algorithms is illustrated in Fig 2.10.

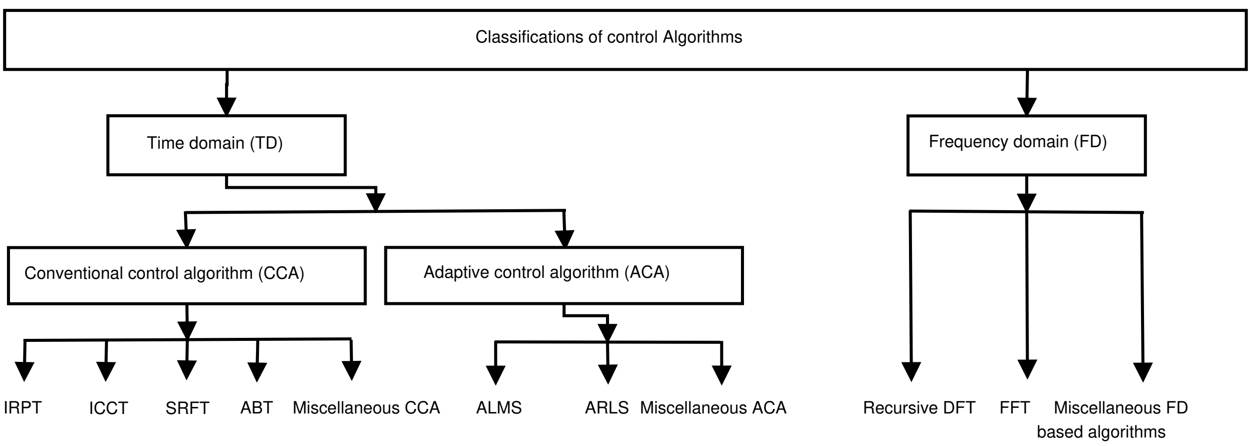

Figure 2.10: General classification of control algorithms.

A general hardware block diagram of these control algorithms are depicted in Fig 2.11. Various functional blocks of control algorithm include sensors, signal conditioning unit, and interface

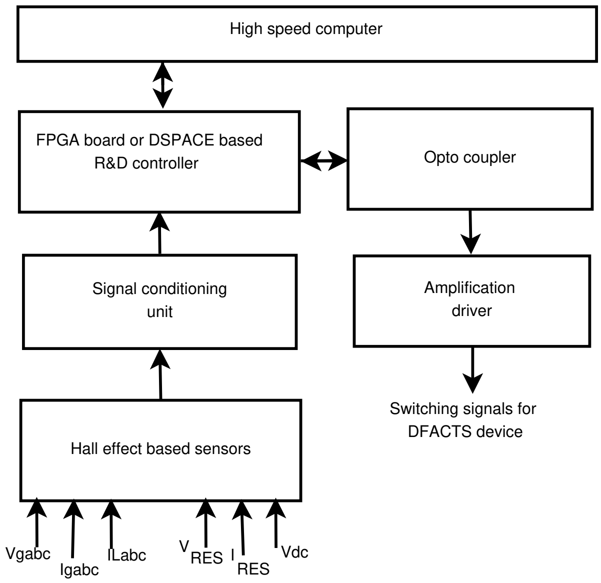

Figure 2.11: Block diagram of the basic experimental framework of control algorithms.

with the high-speed computer through FPGA or dSPACE controller. The high-speed computer processes multiple inputs, including the system data and output switching signals to DFACTS devices via optocoupler and buffers circuit.

2.4.1 Conventional Control Algorithms

Conventional control algorithms work on the concept of 3-phase to 2-phase and 2-phase to the 3-phase transformation of voltage and current signals with a phase-locked loop circuit for the estimation of reference gate signals required to drive the DFACTS devices [Singh and Solanki, 2009]. The design process involved in designing the conventional control algorithm is well explained in [Chawda *et al.*, 2020].

The concept of IRPT was first proposed by H. Akagi and has been used to generate the reference signal for DSTATCOM devices to mitigate PQ issues. The basic working methodology of this theory includes the transformation (3-phase to 2-phase) and reverse conversion (2-phase to 3-phase) of voltage and current quantities for the estimation of reference current signal. The computations involved in the IRPT theory to estimate instantaneous active (p) and reactive (q) components of current signals have been presented in [Murugesan *et al.*, 2015]. In ICCT control theory, 3-phase grid voltages are utilized to compute 3-phase reference currents. These reference currents consist of in-phase component (active component) and out-phase component (quadrature component) as presented in [Bhatia *et al.*, 2005]. The SRFT control theory is based on the sensed load current, and grid voltage signals [Singh *et al.*, 2011a]. In the Admittance based approach, the active (p) and reactive (q) components are estimated using voltage, and current signals of the system [Philip *et al.*, 2015]. The other conventional control algorithms have played an important role in PQ mitigation with DSTATCOM. These includes, power balance control [Singh *et al.*, 2018], instantaneous symmetrical components control [Tummuru *et al.*, 2014], sliding mode control (SMC) [Liu *et al.*, 2012], PLL based control [Voglitsis *et al.*, 2018] and their modified methods. However, the experimental framework for conventional control algorithms has not been extensively used with RE penetration in the utility grid.

It has been reported that the compatibility and performance of conventional control algorithms with RE penetration are not providing good results as expected. Hence, the performance

Table 2.4: Limitations of conventional control algorithms.

S.No.	Limitations
1.	Complex circuitry like PLL is required.
2.	High computation the dynamic response is slow and more complex.
3.	DC link voltage and DSP speed oscillations are high.
4.	Accuracy is medium due to poor stability.
5.	THD calculation is not accurate due to low dynamic response.

of these algorithms is low compared to adaptive control algorithms due to limitations as described in Table Table 2.4. The conventional control algorithms use complex circuitry like PLL, 3-phase to 2-phase conversion blocks, 2-phase to 3-phase conversion blocks. Therefore computational complexity associated with these algorithms is high and dynamic response is slow. Hence, the performance of conventional control algorithms is poor in mitigating the harmonics. However, when these algorithms are burned in the hardware-based R&D controllers like DSP, the oscillations are high in computational speed and DC link voltage.

2.4.2 Adaptive Control Algorithms

Researchers have started switching to adaptive signal processing-based algorithms to enhance the power quality of grid integrated RE sources with DFACTS devices. These control algorithms continuously update the weight component of current and voltage signals based on the initial values, old estimation and system changes for the estimation of reference gate signals. The simplest Least Mean Square (LMS) algorithm was proposed by Widrow et al. [Widrow *et al.*, 1976]. The notability of the LMS algorithm is easy to implement. The implementation of neural network-based LMS controlled VSC for PQ mitigation has been presented in [Singh *et al.*, 2011b]. However, the LMS algorithm becomes unstable with a low signal to noise ratio (SNR). LMF is a fourth-order error correction algorithm, exhibits stability even with low SNR values [Eweda, 2012] as static error and mean square error associated with LMF control is lower compared to LMS algorithm [Agarwal *et al.*, 2016b]. The LMS/F algorithms were found to be classical methods for adaptive system identification (ASI) [Gui *et al.*, 2014]. These algorithms are also used in mobile communication [Otaru *et al.*, 2011]. The details of the implementation of the recursive least-squares algorithm are presented in [Haykin, 2008]. This adaptive algorithm provides better convergence and highly correlated input signals than the LMS algorithm. The price to pay for this is an increase in computational complexity. Variable forgetting factor recursive least-squares (VFFRLS) algorithm has been developed in [Paleologu *et al.*, 2008]. This algorithm has reduced computational complexity and the ability to adopt various changes in the system to obtain desired signals for solving complexity and stability issues [Badoni *et al.*, 2015].

1. **Design of adaptive control algorithm** The various design steps involved in adaptive control algorithms are detailed below. Standard notation and nomenclature are used based on the research articles cited in this thesis.

   - **Estimation of active and reactive unit templates**: 3-phase line voltages (v_{sab}, v_{sbc}) are utilized to obtain phase voltages using the following relation,

     $$\begin{Bmatrix} v_{sa} = (2v_{sab} + v_{sbc})/3 \\ v_{sb} = (-v_{gab} + v_{sbc})/3 \\ v_{sc} = (-v_{sab} - 2v_{sbc)})/3 \end{Bmatrix} \tag{2.1}$$

     Peak amplitude of terminal voltage (v_t) is given as,

     $$v_t = \sqrt{2/3(v_{sa}^2 + v_{sb}^2 + v_{sc}^2)} \tag{2.2}$$

Three-phase in-phase (active) unit vector templates (u_{pa}, u_{pb}, u_{pc}) are given as,

$$u_{pa} = v_{sa}/v_t, u_{pb} = v_{sb}/v_t, u_{pc} = v_{sc}/v_t \tag{2.3}$$

Three-phase quadrature (reactive) unit templates (u_{qa}, u_{qb}, u_{qc}) are given as,

$$\begin{Bmatrix} u_{qa} = -u_{pb}/\sqrt{3} + u_{pc}/\sqrt{3} \\ u_{qb} = \sqrt{3}u_{pa}/2 + (u_{pb} - u_{pc})/2\sqrt{3} \\ u_{qc} = -\sqrt{3}u_{pa}/2 + (u_{pb} - u_{pc})/2\sqrt{3} \end{Bmatrix} \tag{2.4}$$

- **Estimation of loss components**: PI voltage regulator is used to generate the active and reactive loss components. Reactive loss component (W_{cq}) is utilized to maintain terminal voltage at PCC.

$$W_{cq}(n+1) = W_{cq}(n) + k_{pq}(v_{te}(n+1) - v_{te}(n)) + k_{iq}v_{te}(n+1) \tag{2.5}$$

Where, $W_{cq}(n+1)$ and $v_{te}(n+1)$ are updated reactive loss component and voltage error. The current value of this voltage error is computed as,

$$v_{te}(n) = v_{tn}(n) - v_t(n) \tag{2.6}$$

This regulator maintains dc link voltage by generating active loss component $(W_{cp)}$.

$$W_{cp}(n+1) = W_{cp}(n) + k_{pd}(v_{de}(n+1) - v_{de}(n)) + k_{id}v_{de}(n+1) \tag{2.7}$$

Where, $W_{cp}(n+1)$ and $v_{de}(n+1)$ are the updated active loss component and dc voltage error. The current value of this dc voltage error is,

$$v_{de}(n) = v^*_{dc}(n) - v_{dc}(n) \tag{2.8}$$

Where, v^*_{dc}; reference DC bus voltage calculated as $(v^*_{dc} = 2\sqrt{2}v_{LL}/\sqrt{3}m)$. v_{LL} represents voltage (line to line) at PCC, m is modulation index. v_{dc}; actual DC link voltage.

- **Estimation of feed forward term**: The feed forward term (W_{RES}) is computed based on current output power (P_{RES}) of RES given by,

$$W_{RES}(n) = 2P_{RES}(n)/3v_t \tag{2.9}$$

- **Extraction of fundamental weight component of load current**: The extraction of active and reactive weight component of load current depends on weight updation methodology used in the control algorithms. Let, the basic load current equation of AC distribution network is given as,

$$i_L(t) = Isin(wt + \phi) + \Sigma I_n sin(nwt + \phi_n) \tag{2.10}$$

It can also be represented as,

$$i_L(t) = i(t) + i_h(t) = i_p(t) + i_q(t) + i_h(t) \tag{2.11}$$

where, $i(t)$ is the fundamental current component which is made up of active current $i_p(t)$ and reactive current $i_q(t)$ whereas $i_h(t)$ is the harmonic current components.

The initial estimation of the active, reactive part of load current and harmonic parts of load current for a single-phase is given as,

$$i_p(t) = W_p \times u_p, i_q(t) = W_q \times u_q \tag{2.12}$$

$$i_h(t) = i_L(t) - i_p(t) - i_q(t) \tag{2.13}$$

The weights (W_p) and (W_q) are not constant values, and continuously update according to the changes associated with system. Active unit voltage template (u_p) and reactive unit voltage template (u_q) are calculated using grid voltages.

- **Estimation of total active and reactive weight components**: The total active weight component (W_{sp}) is calculated by adding dc loss component (W_{cp}) to average active weight component (W_{Lpa}) and deducting the feed-forward RES weight component (W_{RES}),

$$W_{sp} = W_{Lpa} + W_{cp} - W_{RES} \tag{2.14}$$

Where,

$$W_{Lpa} = (W_{pa} + W_{pb} + W_{pc})/3 \tag{2.15}$$

Similarly, the total reactive weight component (W_{sq}) is calculated by subtracting the average reactive weight component (W_{Lqa}) to the ac loss component (W_{cq}),

$$W_{sq} = W_{cq} - W_{Lqa} \tag{2.16}$$

Where,

$$W_{Lqa} = (W_{qa} + W_{qb} + W_{qc})/3 \tag{2.17}$$

- **Generation of three-phase reference signals**: The active reference signal (i^*_{pabc}) is estimated using total active weight component (W_{sp}) and 3-phase active unit templates.

$$i^*_{pabc} = W_{sp} \times u_{pabc} \tag{2.18}$$

Similarly, the reactive reference signal (i^*_{qabc}) is estimated using reactive weight component (W_{sq}) and 3-phase active unit templates.

$$i^*_{qabc} = W_{sq} \times u_{qabc} \tag{2.19}$$

Thus, 3-phase reference grid current signals are generated by combining active reference signal (i^*_{pabc}) and reactive reference signal (i^*_{qabc}),

$$i^*_{sabc} = i^*_{pabc} + i^*_{qabc} \tag{2.20}$$

Note: The details of the reference current generation may vary with the type of algorithm.

- **Generation of gating signals**: The generated 3-phase reference signals (i^*_{sabc}) along with actual grid signals (i_{sabc}) are fed to pulse width modulation based controller to generate gating signals for DFACTS devices.

Note: The gating signals for the fourth leg switches of DFACTS device in 3P4W utility grid are calculated from the current error signal by comparing sensed neutral signal (i_{sn}) and reference neutral current signal (i^*_{sn}). These current signals are calculated as,

$$\begin{Bmatrix} i^*_{sn} = 0 \\ i_{sn} = -(i_{sa} + i_{sb} + i_{sc}) \end{Bmatrix} \tag{2.21}$$

State of the art establishes that adaptive signal processing-based control algorithms provide ease for estimating the active component and reactive component and adaptiveness. These algorithms exhibit robustness and faster response. The performance of various conventional and adaptive control algorithms are analyzed by selecting different parameters of these algorithms used in recent research as listed in Table 2.5. However, Table 2.6 shows the experimental data-based performance analysis of these algorithms. In Table 2.6, parameters are selected based on the laboratory-based experimental data from the respective references. It can be perceived from

Table 2.5: Performance analysis of various control algorithms for PQ improvement.

Parameters	Conventional Control Algorithms				Adaptive Control Algorithms		
	ICCT	IRPT	SRFT	Admittance	Adaline	ALMS	ARLS
Nature of Controlling	Non-adaptive	Non-adaptive	Non-adaptive	Non-adaptive	Adaptive	Adaptive	Adaptive
Reactive power compensation	Average	Good	Good	Very Good	Very Good	Excellent	Excellent
Harmonic mitigation	Average	Average	Good	Good	Very Good	Excellent	Excellent
Power factor correction	Average	Good	Very Good	Good	Excellent	Excellent	Excellent
Load balancing	Good	Good	Good	Good	Good	Very Good	Good
Neutral current elimination	Good	Good	Very Good	Good	Good	Very Good	Very Good
Voltage regulation	Average	Average	Good	Good	Good	Excellent	Good
Robustness	Poor	Poor	Good	Average	Very Good	Excellent	Excellent
Flexibility	Poor	Poor	Good	Average	Very Good	Excellent	Good
Convergence	-	-	-	-	Good	Excellent	Excellent
Performance with RES	Poor	Poor	Good	Good	Very Good	Excellent	Excellent
Computational complexity	Poor	Poor	Average	Poor	Average	Average	Average

Table 2.6: Performance analysis of various control algorithms based on experimental datas.

Parameters	SRFT	LMS	LMF	VSLMS	ANFIS LMS	RLS	VFFRLS
	[Agarwal *et al.*, 2016b]			[Badoni *et al.*, 2016]		[Badoni *et al.*, 2015]	
Type	Time domain PLL based	Adaptive filter	Adaptive filter	Stochastic gradient	-	Least square estimation	Least square estimation
Input signal	-	Stochastic	Stochastic	Stochastic	Stochastic	Deterministic	Deterministic
Computation complexity	High	Low	Low	High	Low	Less	Moderate
Order of optimization	-	2^{nd} order	4^{th} order	-	-	-	-
Static error	-	More	Less	Medium	Less	Less	Less
Dynamic response	Slow	Medium	Fast	Fast	Fast	Medium	Fast
MSE	-	19.79	17.02	-	-	-	-
Computations	More	Less	Less	Less	Less	Less	Less
DSP speed	High	Low	Low	Low	Low	Medium	Low
Convergence rate	-	Oscillate at mean value	Oscillate at mean value	Oscillate at mean value	0.1 s	Oscillate at mean value	0.15 s
Sampling time	-	50 μ s	50 μ s	60 μ s	60 μ s	50 μ s	60 μ s
Step size	-	Fix	-	Variable	Variable	Fix	Variable
Accuracy	Poor	Medium	High	High	High	Medium	High
Stability	-	Good	Better	Good	Better	Good	Better
THD (%)	- -	$i_s = 4.29$ $i_L = 26.66$	$i_s = 1.12$ $i_L = 27.24$	$i_s = 3.62$ $i_L = 26.66$	i_s =2.57 $i_L = 26.7$	$i_s = 3.68$ $i_L = 26.95$	$i_s = 2.44$ i_L =26.95

the tabled data that the implementation of adaptive control algorithms was found comfortable with *R&D* controllers. The output of these algorithms is superior compared to the conventional control algorithms. In addition to the above, the compatibility and performance of adaptive control algorithms with RE penetration provide better results. The performance comparison of the 3P3W and 3P4W systems in RE penetration is presented in Table 2.7. This table aims to incorporate recent research in the area of PQ mitigation. For this purpose, tabled data shows the system parameters, reference signal generation algorithms, voltage regulation devices, comparators for PWM generators, and DFACTS devices used for various research in different applications. The study on critical factors is also essential for WE penetration in the rural grid with feasibility and economic considerations. These factors and their illustrations are presented in Table 2.8.

Table 2.7: Performance analysis of 3P3W and 3P4W utility grid with RE penetration.

Achievements	System	RSGA	Regu lator	Compa rator	DFACTS devices	References
Mitigation of various PQ issues under unbalanced NL-loads and supply active power as required has been achieved.	3P4W: PSMG-2.5KW, Grid-30V,60Hz	IRPT	PI	HCC	VSC	[Singh *et al.*, 2010]
DC-link voltage has been maintained to control the power flow of the SPV system by compensating reactive power under the N-L load.	3P3W: PV Array Grid 230V, 50 Hz	SRF and IRPT	PI	SMC	VSC	[Mishra and Ray, 2016]
The inverter is actively compensated for the current imbalance harmonics and reactive power for smooth bidirectional power flow.	3P4W: PMSG-2.5KW, Grid 30V, 60Hz	ANFIS	PI	HCC	VSC	[Singh and Chandra, 2013]
Smooth SPV integration and balancing of loads have been achieved using Normalized-LMS (NLMS).	3P3W: SPV-8.1kW, Grid 415V, 50 Hz	NLMS	PI	PWM	VSC	[Agarwal *et al.*, 2016a]
Mitigation of various PQ issues under different dynamics and steady-state operating conditions.	3P4W: SPV-30KW Grid 415V, 50Hz	ANF	PI	PWM	VSC	[Singh *et al.*, 2016]
Harmonics elimination, PF correction, load balancing, voltage fluctuations, compensation of reactive power, under N-L loads have been achieved using variable step-size least mean fourth (VSS-LMF) algorithm.	3P3W: SPV-6.8kW Grid 415V, 50Hz	VSS-LMF	PI	PWM	VSC	[Agarwal *et al.*, 2016c]
Mitigation of harmonics, reactive power, and neutral current compensation has been achieved and maintain balanced grid currents using Second Order Generalized Integrator-Quadrature (SOGI-Q).	3P4W: SPV-7kW Grid 415V, 50Hz	SOGI-Q	PI	HCC	VSC	[Jain and Singh, 2017]
PQ issues are mitigated under the Wind speed variations.	3P4W: DFIG-3.7kW Grid 415V, 50Hz	PLL based	PI	PWM	VSC	[Naidu and Singh, 2017]
Elimination of current harmonics and provides load balancing with controlled terminal voltage.	3P3W: SPV-6.8kW, Grid 415V, 50Hz	PLL-lesss	PI	PWM	VSC	[Agarwal *et al.*, 2017b]
Compensate the various PQ issues such as reactive power under NL load using conservative power theory (CPT).	3P4W: PMSG-10KW Opal RT	CPT	PI	SPWM	VSC	[Bubshait *et al.*, 2017]
The need for additional power converters for PQ mitigation studies has been avoided by using the proposed structure.	3P3W: RES inverter-5kVA, Grid 415V	ANF	PI	PWM	VSC	[Chilipi *et al.*, 2017]
Various PQ issues have been mitigated, and the proposed system effectively transfers active power from the PV array to the local loads, and the grid using decorrelation normalized least mean square (DNLMS) algorithm.	3P3W: SPV-5.36kW Grid 227Vrms, 50Hz	DNLMS	PI	HCC	VSC	[Pradhan *et al.*, 2018]
The LMF control is found more effective then LMS control in terms of minimization of mean square error and static error for PQ mitigation.	3P3W: SPV-8kW, Grid 415V, 50Hz.	LMF	PI	PWM	VSC	[Agarwal *et al.*, 2016b]
Low mean square error, fast converges and improved PQ have been achieved.	3P4W: SPV-54kW, Grid 415V, 50Hz	Modified LMF	PI	PWM	VSC	[Beniwal *et al.*, 2016]

Table 2.8: Feasibility and economic consideration of grid tied WE source.

Factors	Illustration
Grid integration	There is no requirement of large-capacity batteries in grid tied WES with DSTATCOM. For similar loads, grid-tied system use smaller WES compare to stand-alone systems.
Distance to utility network	Grid-tied WES with DSTATCOM should be integrated into utility grid as nearest as possible to avoid unnecessary operations. Stand-alone systems have a big issue, as it is located far from electrical utility networks, which is uneconomical. Distance is increasing losses are also increases with the length of the line.
Balance of system components	International safety standards and regulations may require a new balance of 3P3W and 3P4W utility system. Initial costs for installation are depending on the balance of system components.
Installation cost	Per watt basis, large scale grid-tied WES with DSTATCOM tend to be economical. This system endows lower initial cost with the energy costs for heavy loads.
Maintenance	There are no moving parts in small scale grid-tied WES with DSTATCOM, so substantial maintenance costs is zero percent.
Energy use and cost	Energy use is a crucial factor in deciding system size. Reducing energy consumption due to small WES with DSTATCOM dramatically reduces the initial capital cost investment.

2.5 NEED OF ADDITIONAL DSTATCOM INFRASTRUCTURE

The DFIG based WE sources need reactive power support when connected at the weak ends of the grid. This system is generally not designed to transfer electrical energy into the rural grids. The length of the feeders are long and operated at a low/medium voltage level characterized by low SCR conditions in the rural grid. Under the conditions of high capacities of DFIGs connected to the rural grid in the presence of NL loads, voltage instability and power losses are possible due to PQ and high reactive power requirements. The built-in converter of DFIG can not meet the reactive power requirements due to the rating inadequacy, and capacity limitations [Hatziargyriou *et al.*, 2020]. These limitations may also restrict the performance of control schemes of DFIG to inject the demanded reactive power during the higher penetration levels of the WE source connected to low SCR-based grids. The possibility of voltage collapse is anticipated in [Mokryani *et al.*, 2012] due to the inadequate capability to inject required reactive power by the built-in converter with appropriate control. The research studies in [Zhang *et al.*, 2009; Durrant *et al.*, 2003] demonstrate that the power injection capabilities for a weak grid ($SCR \leq 3$) and ultra-weak grid ($SCR < 2$) are limited due to the reactive power requirement. In addition, the power transfer limits imposed on the WE source connected to weak grids may also result in instability problems [Li *et al.*, 2019b]. Therefore, modern WE sources must meet technical requirements such as reactive power capability, low voltage ride through, and PQ issues during high WE penetration levels. In [Chi *et al.*, 2019], the authors proposed an additional DSTATCOM based infrastructure with coordinated VAR planning for maintaining voltage stability during high WE penetration. However, keeping the voltage stability beyond 20%, WE penetration is challenging for the weak grid with precise planning requirements of reactive power and PQ mitigation strategy [Zhou *et al.*, 2005].

Thus, an additional DSTATCOM based reactive power compensator is required to adjust the generation or absorption of fast reactive power in response to a control signal. Injecting the reactive power at the PCC can maintain the voltage in the stability range at high WE penetration [C-2, 2019]. Therefore, the purpose of DSTATCOM is to regulate the voltage of the system during high WE penetration and improve PQ. The performance of DSTATCOM is majorly dependent on the control algorithm. The power quality is effectively mitigated by implementing DSTATCOM for specific applications such as stand-alone and grid-tied wind, solar and hybrid power generation, rural and metropolitan electric power network, distribution load compensation, water pumping systems, etc [Gandoman *et al.*, 2018; Hingorani and Gyugyi, 2000]. The major reasons which show the need for additional DSTATCOM infrastructure for PQ improvement are as follows:

2.5.1 Limitations of Built-in Converter in DFIG based WE system

The block diagram and details of the Type-3 DFIG-based WECS system is presented in Subsection 2.2 and Fig.2.3, respectively.

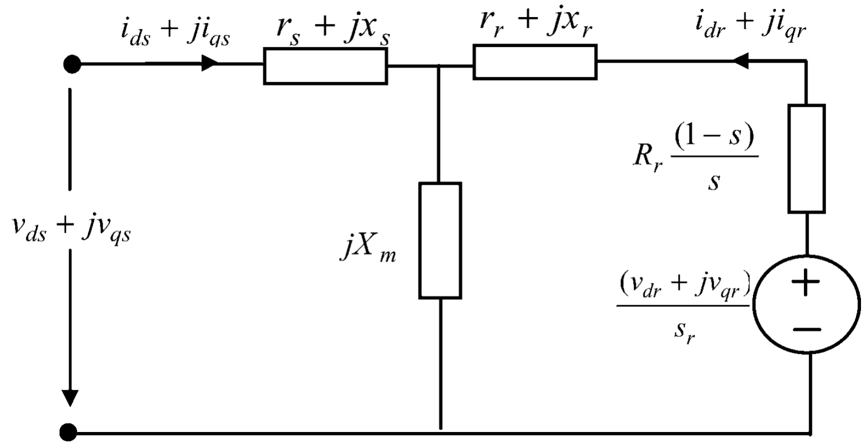

Figure 2.12: Equivalent circuit of DFIG wind turbine.

1. **Equivalent Circuit of DFIG:** [Wu *et al.*, 2008] et al. presented the equivalent circuit diagram of DFIG, which is illustrated in Fig. 2.12. The dynamic equations of DFIG is written as,

$$2H_{total}\frac{ds}{dt} = P_s - P_m \tag{2.22}$$

$$\frac{dE_q{'}}{dt} = -s\omega_s E_d^{'} + \omega_s \frac{L_m}{L_{rr}} v_{dr} - \frac{1}{T_0^{'}}[E_q^{'} - (X_s - X_s^{'}) i_{ds}] \tag{2.23}$$

$$\frac{dE_d^{'}}{dt} = -s\omega_s E_q^{'} + \omega_s \frac{L_m}{L_{rr}} v_{qr} - \frac{1}{T_0^{'}}[E_d^{'} - (X_s - X_s^{'}) i_{qs}] \tag{2.24}$$

where,

$$X_s = \omega_s L_{ss} = x_s + X_m \tag{2.25}$$

$$X_s^{'} = \omega_s (L_{ss} - L_m^2 / L_{rr}) \tag{2.26}$$

$$T_0^{'} = L_{rr}/R_r \tag{2.27}$$

Likewise, the electrical equations is written as,

$$P_s = -E_d^{'} i_{ds} - E_q^{'} i_{qs} \tag{2.28}$$

$$Q_s = E_d^{'} i_{qs} - E_q^{'} i_{ds} \tag{2.29}$$

$$E_d^{'} = -r_s i_{ds} + X_s^{'} i_{qs} + v_{ds} \tag{2.30}$$

$$E_q^{'} = -r_s i_{qs} - X_s^{'} i_{ds} + v_{qs} \tag{2.31}$$

s: Rotor slip, H_{total}: Total inertia constant of the turbine and the generator, P_s: Output active power of the stator of the DFIG, P_m: Mechanical power of the WT, L_{ss}: stator self-inductance, L_{rr}: Rotor self-inductance, L_m: Mutual inductance, ω_s synchronous angle speed, X_s: Stator reactance, x_s: Stator leakage reactance, x_r: Rotor leakage reactance, $X_s^{'}$: Stator transient reactance, $E_d^{'}$ and $E_q^{'}$ are the d and q axis voltages behind the transient reactance, respectively. $T_0^{'}$ Rotor circuit time constant, i_{ds} and i_{qs} are the d and q axis stator currents, respectively. v_{ds} and v_{qs} are the d and q axis stator terminal voltages, respectively. v_{dr} and v_{qr} are the d and q axis rotor voltages, respectively. Q_s is the reactive power of the stator of the DFIG. Equations 2.25, 2.26, and 2.27 shows the third-order DFIG model and the voltage equations and the flux linkage equations of the DFIG are based on the motor convention. From equations 2.26 and 2.27 the model of the WT with DFIG is a system with two inputs in the d-q reference frame [Wu *et al.*, 2008]. The inputs are v_{dr} and v_{qr}, respectively.

2. **Capability Limits of DFIG:** The stator and rotor rated current are majorly responsible for the heating of the stator and the rotor windings due to Joule losses. Thus, DFIG capability limits in the steady-state condition are obtained. Further, it can also be calculated through the total capacity limits of WT [Montilla-DJesus *et al.*, 2012; Latran *et al.*, 2015].

   a) **Stator Current Limit:** The stator current limit is calculated using the heating due to the Joule's stator winding losses. The per-unit stator current limit is written as,

$$P_s^2 + Q_s^2 = 3V_s^2 I_s^2 \tag{2.32}$$

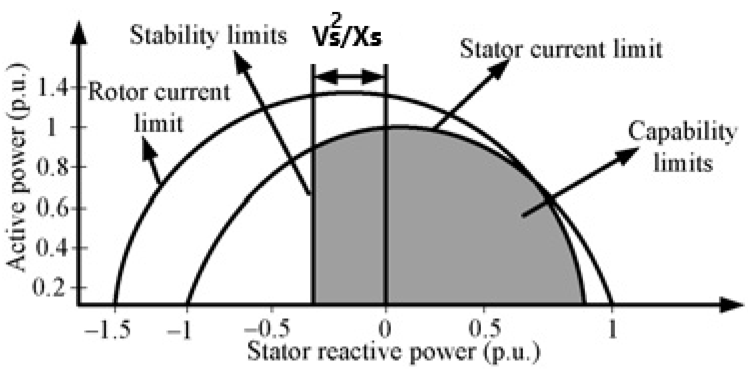

Figure 2.13: Capability limit curves of DFIG wind turbine.

P_s: Stator active power, Q_s: Stator reactive power, V_s: Stator voltage and I_s: Stator current. The steady-state capacity limits of the DFIG are presented in [Mokryani *et al.*, 2012], which is as illustrated in Fig.2.13. The PQ curve shows the minimum absolute value of the stator current, the rotor current, the maximum active power, and the stability limits. The shaded area represents the feasible area of operation for the DFIG based wind turbine. It can be observed from Equation2.32 that the locus of the maximum stator current in the PQ plane is a circle centred at the origin, with a radius equal to the apparent power of the stator [Mokryani *et al.*, 2012].

b) **Rotor Current Limit:** The rotor current limit is calculated using the heating due to the Joule's losses of the rotor winding [Mokryani *et al.*, 2012]. Therefore, the stator active and reactive power is calculated concerning rated stator voltage,

$$P_s = \frac{X_m}{X_s} V_s I_r sin\delta \tag{2.33}$$

$$Q_s = \frac{X_m}{X_s} V_s I_r cos\delta \frac{V_s^2}{X_s} \tag{2.34}$$

c) **Total Capability Limits:** The addition of rotor P_r and stator P_s active power gives total active power P_{Total} of the DFIG [Mokryani *et al.*, 2012]. It is written as,

$$P_{Total} = P_s + P_r \tag{2.35}$$

$$P_r = -SP_s \tag{2.36}$$

$$P_t = (1 - S)P_s \tag{2.37}$$

d) **Min-Max Reactive Power Limits:** Min-Max reactive power limits are obtained by simplification of equations 2.33 and 2.34.

$$P_s^2 + \left(Q_s + \frac{V_s^2}{X_s}\right)^2 = \left(\frac{X_m}{X_s} V_s I_r\right)^2 \tag{2.38}$$

With reference to Fig.2.14, Equation 2.38 illustrates a circle centered at $[-(V_s^2/X_s), 0]$ with a radius equal to $[(X_m/X_s)V_s I_r$. The stator's active and reactive power is written to function the maximum allowable rotor and stator current [Mokryani *et al.*, 2012; Montilla-DJesus *et al.*, 2010].

$$P_s^2 + Q_s^2 = 3V_s^2 I_s^2 \tag{2.39}$$

$$P_s^2 + \left(Q_s + \frac{V_s^2}{X_s}\right)^2 = \left(3\frac{X_m}{X_s} V_s I_r\right)^2 \tag{2.40}$$

A circumference centered equal to the stator rated apparent power is presented in Equation 2.39 and a circumference centered at $[-3(V_s^2/X_s), 0]$ is presented in Equation 2.40. However, substituting Equations 2.36 and 2.37 into Equations 2.39 and 2.39 can be written as,

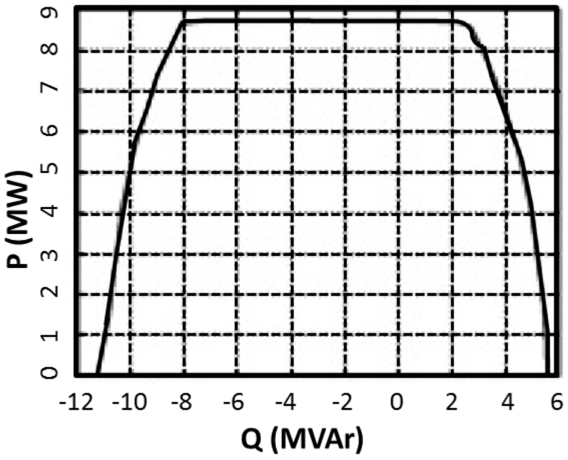

Figure 2.14: Capability curve of a 9 MW Wind Farm under normal operation.

$$\left(\frac{P_t}{1-S}\right)^2 + Q_t^2 = (3V_sI_s)^2 \tag{2.41}$$

$$\left(\frac{P_t}{1-S}\right)^2 + \left(Q_t + \frac{V_s^2}{X_s}\right)^2 = \left(3\frac{X_m}{X_s}V_sI_r\right)^2 \tag{2.42}$$

The maximum currents of the stator (I_{smax}) and rotor I_{rmax} helps to achieve the capability limits of DFIG using Equations 2.41 and 2.42.

[Mokryani *et al.*, 2012] et al. discussed the standard capability curve of a 9 MW Wind Farm, which is as illustrated in Fig.2.14. The DFIG based WT can inject 2.5 MVAr or absorb -8 MVAr, which shows the reactive power limits for 9MW WE source. The built-in converter control scheme of the WECS source suffers from the limitations associated with the DFIG based WT. The performance is further degraded under the various strength of the ac grid and the proliferation of non-linear loads. Hence, these aspects have also been considered in this research work, and integrating additional DSTATCOM with an adaptive control algorithm mitigates the limitations mentioned above.

2.5.2 Rural Grid

In the case of rural grids (weak grids), the reactive power support required is substantially large. Hence the built-in converter of wind energy conversion system may fail to meet the reactive power demand unless it is considered in the design of the converter. Failing to provide the required reactive power supply by a built-in converter may lead to voltage instability and other PQ disturbances [Li *et al.*, 2019b]. This leads to the limited power injection capability of the WE generator. The research studies in [Zhang *et al.*, 2009; Durrant *et al.*, 2003] demonstrate that the power injection capabilities in a weak grid (SCR$\leq$3) and ultra-weak grid (SCR<2) are limited due to the PQ issues such as continuous power variations, voltage variations, flicker, harmonics and reactive power.

The Short Circuit Ratio defines the strength of the AC grid, which can be expressed as:

$$SCR = S_{cc}/S_p \tag{2.43}$$

Where S_{cc} is the short circuit power of the grid at the PCC, expressed as $S_{cc} = V_g^2/|Z_g|$, and S_p is the rated generation power of the total WE sources. Likewise, the SCR is estimated as,

$$SCR = V_g^2/(|Z_g|S_p) \tag{2.44}$$

Where V_g is rated voltage, and $|Z_g|$ is grid impedance. If the SCR is ≤ 3 grid is set to be weak, if the SCR is < 2 then it is termed as ultra-weak grid and if the value of SCR is > 5, it is known as a stiff grid [Yang *et al.*, 2019].

2.5.3 Wind Energy Penetration Levels

Most WE sources employ Induction Generators (IG) to convert wind energy to electrical energy. These are connected to ac grid through a built-in converter. IGs need reactive power support for their successful operation, which is provided by the built-in converter, generally controlled by the conventional vector control schemes. It also helps in mitigating the PQ disturbances associated with WE (intermittency and uncertainty) [Shafiullah, GM and Oo, Amanullah MT and Ali, ABM Shawkat and Wolfs, Peter, 2013]. Mitigation of PQ issues like voltage stability, harmonics, and flickers by built-in converter with vector control has been reported in [Kaddah *et al.*, 2016]. The system considered for this case study has 10% of WE penetration in a grid of SCR 10. A built-in converter's failure to provide the required reactive power supply may lead to voltage instability and other PQ disturbances, significantly limiting wind energy penetration levels. The research studies at the ERCOT test bench proved that the power injection capability is limited to 13% in the case of a grid with an SCR of 2 [Huang *et al.*, 2012]. Zhou et al. [Zhou *et al.*, 2005] presented various case studies and established that maintaining the voltage stability beyond 20% of WE penetration is a big challenge in the case of a weak grid owing to PQ. Hence, researchers suggested an additional converter with an appropriate control technique (at the PCC) to meet the challenges of large WE penetration in a weak ac grid [Chen *et al.*, 2009]. Chi et al. [Chi *et al.*, 2019], suggested an additional DSTATCOM at PCC to achieve a penetration level of 20 to 30% in the presence of light and induction motor loads at PCC.

The WE penetration (WEP) level into the AC grid is defined as; it is the ratio of total installed WE capacity to peak load on the system with appropriate power loss [Mosaad, 2018].

$$WEP(\%) = \frac{P_C}{P_L} \tag{2.45}$$

P_C is the total installed power capacity of WE (MW), and P_L is connected peak load (MW).

2.5.4 Unbalanced/Non-linear loads

The unbalanced loads of a three-phase line are generated due to the unequal three-phase line, or open-circuited one-two phase of a line. These loads cause unbalanced 3-phase currents, which raises an unstable 3-phase terminal voltage. Also, in the case of NL loads, the current signal contains harmonics and significantly deteriorate the system's PQ [Liu *et al.*, 2020b]. Consequently, weak ac grids in the presence of these loads can pose severe PQ disturbances and limit the wind penetration levels at PCC. Otchere *et al*. [Otchere *et al.*, 2020], investigated the voltage stability of grid SCR equal to 5 with considering WE of 10-40 % in the presence of 0.8-lag PF loads. This investigation illustrated that proper reactive power injection management strongly needs to consider the connected loads. The connect loads, especially non-linear loads, may also considerably impact a higher wind power penetration level.

2.6 DISTRIBUTION STATIC COMPENSATOR (DSTATCOM)

The Static Synchronous Compensator (STATCOM) is a voltage source converter connected in shunt to the source for improving power quality with appropriate control [Chandra *et al.*, 2000]. It draws a negligible amount of real power to keep DC-link voltage at its reference value and inject reactive power according to the demand. This compensator used in the distribution system is called Distribution-STATCOM (DSTATCOM) [Singh *et al.*, 2014]. The reactive power output is a linear function of the voltage, and it is the most desirable alternative for providing dynamic reactive power support [Gounder *et al.*, 2016].

The grid code compliance missing functionality to WE sources is filled by developing medium voltage DSTATCOM technology in [Chandra *et al.*, 2000]. It serves as a pure static device and provides excellent steady-state and dynamic operation during the higher WE penetration.

1. **Operating Principle of DSTATCOM:** The idea of DSTATCOM has been identified and is detail reported in CIGRE publication no. 144 in [Erimez and Foss, 2000]. The basic diagram is as shown in Fig 2.15. The inductance has represented an interfacing reactor or an interfacing transformer. The concept is that accurate controlling of the voltage amplitude of the DSTATCOM helps control reactive power at the PCC.

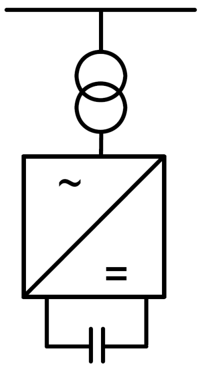

Figure 2.15: Block diagram of DSTATCOM connected to grid.

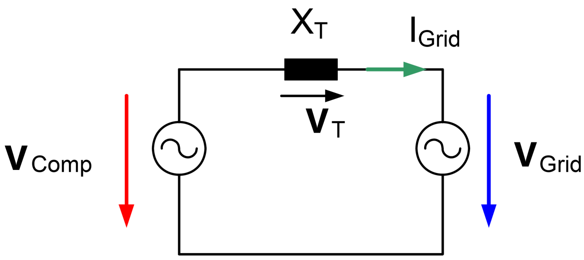

Figure 2.16: Circuit diagram of DSTATCOM.

The single line and phasor diagrams of DSTATCOM illustrate in Fig 2.16 and Fig 2.17, respectively. The basic principle of DSTATCOM can be better understood with the help of these diagrams. If the compensator voltage vector V_{Comp} is higher than the grid voltage vector (V_{Grid}), the DSTATCOM acts as a capacitor as per the definition given in Fig 2.16. The vector of the voltage drop across the inductance (X_T) is visualized in the same direction as the compensator voltage vector. Therefore the compensator current I_{Grid} flows in a positive direction. If the compensator voltage vector (V_{Comp}) is below the grid voltage vector, the DSTATCOM acts like an inductor as per the definition given in Fig 2.16. The vector of the voltage drop across the inductance (X_T) is opposite to the compensator voltage vector.

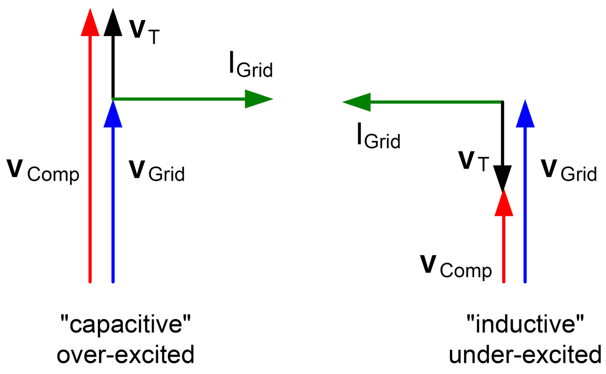

Figure 2.17: Vector diagram for capacitive and inductive DSTATCOM operation.

Therefore the compensator current I_{Grid} flows in the negative direction. In both cases, DSTATCOM power is found to be purely reactive. It can be observed that the current is phase-shifted by 90° compared to the grid voltage [Maibach *et al.*, 2007].

[Saqib and Saleem, 2015] et al. discussed the reactive current versus voltage characteristics of DSTATCOM, which is as illustrated in Fig 2.18. The reactive current is independent of the grid voltage. Therefore, the reactive power changes linearly with the grid voltage.

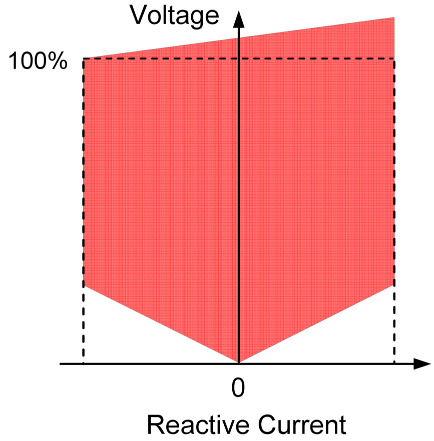

Figure 2.18: Reactive current versus voltage of a DSTATCOM.

2. **Design Consideration of DSTATCOM:** The design considerations of various components of DSTATCOM is presented in below.

   - The reference DC-link capacitor voltage calculation is essential for practical voltage support at PCC, which taken as 680V for all case studies.

     $$v^*_{dcd} = 2\sqrt{2} \times (V_{LL}/\sqrt{3}) \times m \tag{2.46}$$

     Where, V_{LL} is line voltage and m is modulation index.

   - The rating of DSTATCOM DC-link capacitor is,

     $$C_{dc} = ((P_{rated}/v_{dcd})/2) \times \omega \times k(v_{dcrip}) \tag{2.47}$$

     Where, angular frequency is represented by ω and ripple voltage is represented by v_{dcrip}. Also, this voltage is 10% of v_{dcd} and the factor of safety k is considered 10.

- The rating of interfacing inductor is designed as,

$$L_f = \sqrt{3} \times m \times \ v_{dcd} \times k/12 \times h \times f_s \times \Delta i \tag{2.48}$$

The switching frequency (f_s) and overloading factor (h) are considered as 20 kHz and 1.2, respectively. Δi is the current ripple and considered as 10% of peak current. The factor of safety k is selected as 15% of v_{dcd}.

- The ripple filter is designed with an appropriate factor of safety based on the switching frequency (f_s). This filter offers a low impedance pathway for the switching ripples. The capacitance (C_f) is calculated as 5 μF for 5 Ω series resistor (R_f) ,

$$R_f \times C_f \leq 1/(4 \times 0.5 f_s) \tag{2.49}$$

- The voltage rating of IGBT is evaluated as,

$$V_{IGBT} = k(v_{dcd} + v_{overshoot}) \tag{2.50}$$

For a peak overshoot ($v_{overshoot}$) of 3%, the rating of V_{IGBT} is 700 V. However, the current rating of IGBT is,

$$I_{IGBT} = k(I_{peak} + I_{ripple}) \tag{2.51}$$

$$I_{peak} = P_{rated}/\sqrt{3} \times V_{PCC} \tag{2.52}$$

I_{ripple} is selected 3% of I_{peak} under NL load condition.

Note: The rating of DSTATCOM is dependent on the connected loads, duration of faults, grid code requirements, and reactive power [Muyeen, 2014]. [Mosaad, 2018] *et al.*, suggested that the DSTATCOM rating can be equal to 30% to 100% of the wind energy capacity.

2.7 IDENTIFIED RESEARCH GAPS

Based on the critical reviews of the articles cited in this chapter, the following are the significant research gaps that need to be explored. These identified research areas have been considered for the research work presented in this thesis.

- Research work reported in the literature established that maintaining the PQ beyond 20% of WE penetration level is a big challenge in the case of a rural (weak) grid due to the reactive power limitation of the built-in converter.

- A lot of research has been reported in the literature targeting the enhancement of WE penetration with the help of different case studies. These case studies are found to address the individual challenges associated with low SCR, presence of NL loads, load unbalancing, etc.

- The challenges associated with wind energy penetration in the rural grid in the combined scenarios of variation in wind speed, variations in SCRs and presence of NL loads need to be addressed.

- Adaptive control algorithms can adapt to the changes associated with wind speed, weak ac grid, and non-linear loads to mitigate PQ and penetration levels. Therefore, design implementation and experimental investigations are required to establish these algorithms' performance for power quality mitigation.

- The experimental investigation of adaptive control algorithms for enhancing WE penetration levels with combined scenarios strongly needs to accomplish to establish the same.

2.8 CONCLUSIONS

This chapter presents the power quality challenges, solutions and international standards associated with renewable energy, especially wind energy sources. It can be concluded that beyond the 20% WE penetration is a significant challenge in the rural grid complying with PQ standards. The reported research illustrates that Doubly Fed Induction Generator (DFIG) is an advanced wind turbine used in the wind energy conversion system because it has low investment and flexible control characteristics. However, DFIG-based wind turbine has reactive power capability limits, limiting the penetration levels in the low SCR grids. The performance of DFIG is also majorly affected under the conditions of variations in the wind speed, grid strength and connected loads due to the power quality and reactive power inadequacy. Therefore additional DSTATCOM structure can help to improve power quality and inject an appropriate amount of reactive power. The adaptive control algorithms have the potential for accurate reactive power planning and optimal switching of DSTATCOM. The research gaps are identified based on the presented literature review.